

A spatial model for rare binary events

July 21, 2016

1 Introduction

The goal in binary regression is to relate a latent variable to a response using a link function. Two common examples of binary regression include logistic regression and probit regression. The link functions for logistic and probit regression are symmetric, so they may not be well-suited for asymmetric data. An asymmetric alternative to these link functions is the complementary log-log (cloglog) link function. More recently, Wang and Dey (2010) introduced the generalized extreme value (GEV) link function for rare binary data. The GEV link function introduces a new shape parameter to the link function that controls the degree of asymmetry. The cloglog link is a special case of the GEV link function when the shape parameter is 0. Although this link was selected due to its ability to handle asymmetry, the GEV distribution is one of the primary distributions used for modeling extremes. Because extreme events are rare, it is therefore reasonable to use similar methods when analyzing rare binary data.

Spatial logistic and probit models commonly employ a hierarchical model assuming a latent spatial process [citation](#). In the hierarchical framework, spatial dependence is typically modeled with an underlying latent Gaussian process, and conditioned on this process, observations are independent. However, if the latent variable is assumed to follow a GEV marginally, then a Gaussian process may not be appropriate to describe the dependence due to the fact that Gaussian processes do not demonstrate asymptotic dependence, except in the case of perfect dependence.

We propose using a latent max-stable process (de Haan, 1984) because it allows for asymptotic dependence. The max-stable process arises as the limit of the location-wise maximum of infinitely many spatial processes. Max-stable processes are extremely flexible, but are often challenging to work with in high di-

mensions (Wadsworth and Tawn, 2014; Thibaud and Opitz, 2015). To address this challenge, methods have been proposed that implement composite likelihood techniques for max-stable processes (Padoan et al., 2010; Genton et al., 2011; Huser and Davison, 2014). As an alternative to these composite approaches, Reich and Shaby (2012) present a hierarchical model that implements a low-rank representation for a max-stable process. Although composite likelihoods have been used to model binary spatial data (Heagerty and Lele, 1998), we chose to use the low-rank representation of a max-stable process given by Reich and Shaby (2012).

Paragraph outlining the structure of the paper

2 Spatial dependence for binary regression

Following Wang and Dey (2010), we propose using the link function based on the GEV distribution (see Appendix A.1). Because the link function is related to the GEV distribution function, we propose to model spatial dependence using a max-stable process (de Haan, 1984) instead of a Gaussian process. Let $Y(\mathbf{s})$ be the observation at spatial location \mathbf{s} in a spatial domain of interest $\mathcal{D} \in \mathcal{R}^2$. We assume $Y(\mathbf{s}) = I[Z(\mathbf{s}) > 0]$ where $Z(\mathbf{s}) = [1 - \xi \mathbf{X}(\mathbf{s})\beta]^{1/\xi}$ is a latent max-stable spatial process. The max-stable process $Z(\mathbf{s})$ has unit Fréchet marginal distribution for each spatial location. It is possible to also incorporate a scale parameter in the expression for $Z(\mathbf{s})$, but we fix the scale to be 1 due to identifiability concerns. Although β and ξ could be permitted to vary across space, we assume that they are constant across \mathcal{D} . At spatial location \mathbf{s} , the marginal distribution is $P[Y(\mathbf{s}) = 1] = 1 - \exp\left[-\frac{1}{z(\mathbf{s})}\right]$. This is the same as the marginal distribution given by Wang and Dey (2010).

For a finite collection of locations $\mathbf{s}_1, \dots, \mathbf{s}_n$, denote the vector of observations $\mathbf{Y} = [Y(\mathbf{s}_1), \dots, Y(\mathbf{s}_n)]^T$. The spatial dependence of \mathbf{Y} is determined by the joint distribution of $\mathbf{Z} = [Z(\mathbf{s}_1), \dots, Z(\mathbf{s}_n)]^T$ which is computationally challenging to obtain. Therefore, to incorporate spatial dependence into the model, we con-

sider the hierarchical representation of the process proposed in Reich and Shaby (2012). Consider a set of $A_1, \dots, A_L \stackrel{iid}{\sim} \text{Positive Stable}(\alpha)$ random effects associated with spatial knots $\mathbf{v}_1, \dots, \mathbf{v}_L$. The hierarchical model is given by

$$\mathbf{Z}|A_1, \dots, A_L \stackrel{indep}{\sim} \text{GEV}[\theta(\mathbf{s}), \alpha\theta(\mathbf{s}), \alpha] \quad \text{and} \quad A_l \stackrel{iid}{\sim} \text{PS}(\alpha) \quad (1)$$

where $\theta(\mathbf{s}) = \left[\sum_{l=1}^L A_l w_l(\mathbf{s})^{1/\alpha} \right]^\alpha$, $w_l(\mathbf{s}_i)$ are a set of L weights that vary smoothly across space and determine the spatial dependence structure, and $\alpha \in (0, 1)$ determines the strength of dependence, with α near zero giving strong dependence and $\alpha = 1$ giving joint independence.

Because the latent \mathbf{Z} are independent given the random effects, the binary responses are also conditionally independent. This leads to the tractible likelihood

$$Y_i|A_1, \dots, A_L \stackrel{indep}{\sim} \text{Bern}[\pi(\mathbf{s}_i)] \quad (2)$$

where

$$\pi(\mathbf{s}_i) = 1 - \exp \left\{ - \sum_{l=1}^L A_l \left(\frac{w_l(\mathbf{s}_i)}{z(\mathbf{s}_i)} \right)^{1/\alpha} \right\}. \quad (3)$$

Many weight functions are possible, but the weights must be constrained so that $\sum_{l=1}^L w_l(\mathbf{s}_i) = 1$ for all $i = 1, \dots, n$ to preserve the marginal GEV distribution. For example, Reich and Shaby (2012) take the weights to be scaled Gaussian kernels with knots \mathbf{v}_l ,

$$w_l(\mathbf{s}_i) = \frac{\exp \left[-0.5 (||\mathbf{s}_i - \mathbf{v}_l||/\rho)^2 \right]}{\sum_{j=1}^L \exp \left[-0.5 (||\mathbf{s}_i - \mathbf{v}_j||/\rho)^2 \right]} \quad (4)$$

where $||\mathbf{s}_i - \mathbf{v}_l||$ is the distance between site \mathbf{s}_i and knot \mathbf{v}_l , and the kernel bandwidth $\rho > 0$ determines the

58 spatial range of the dependence, with large ρ giving long-range dependence and vice versa.

59 After marginalizing out the positive stable random effects, the joint likelihood of \mathbf{Z} is given by

$$G(\mathbf{z}) = \exp \left\{ - \sum_{l=1}^L \left[\sum_{i=1}^n \left(\frac{w_l(\mathbf{s}_i)}{z(\mathbf{s}_i)} \right)^{1/\alpha} \right]^\alpha \right\}, \quad (5)$$

60 where $G(\cdot)$ is the CDF of a multivariate GEV distribution. This is a special case of the multivariate GEV
61 distribution with asymmetric Laplace dependence function (Tawn, 1990).

62 **3 Joint distribution**

63 We give an exact expression in the case where there are only two spatial locations which is useful for
64 constructing a pairwise composite likelihood (Padoan et al., 2010) and studying spatial dependence. When
65 $n = 2$, the probability mass function is given by

$$P[Y(\mathbf{s}_i), Y(\mathbf{s}_j)] = \begin{cases} \varphi(\mathbf{z}) & Y(\mathbf{s}_i) = 0, Y(\mathbf{s}_j) = 0 \\ \exp \left\{ -\frac{1}{z(\mathbf{s}_i)} \right\} - \varphi(\mathbf{z}), & Y(\mathbf{s}_i) = 1, Y(\mathbf{s}_j) = 0 \\ 1 - \exp \left\{ -\frac{1}{z(\mathbf{s}_i)} \right\} - \exp \left\{ -\frac{1}{z(\mathbf{s}_j)} \right\} + \varphi(\mathbf{z}), & Y(\mathbf{s}_i) = 1, Y(\mathbf{s}_j) = 1 \end{cases} \quad (6)$$

66 where $\varphi(\mathbf{z}) = \exp \left\{ - \sum_{l=1}^L \left[\left(\frac{w_l(\mathbf{s}_i)}{z(\mathbf{s}_i)} \right)^{1/\alpha} + \left(\frac{w_l(\mathbf{s}_j)}{z(\mathbf{s}_j)} \right)^{1/\alpha} \right]^\alpha \right\}$. For more than two locations, we are also
67 able to compute the exact likelihood when the number of locations is large but the number of events is small,
68 as might be expected for very rare events (see Appendix A.2).

4 Quantifying spatial dependence

Assume that Z_1 and Z_2 are both $\text{GEV}(\beta, 1, 1)$ so that the probability of Y_i decreases to zero as β increases.

A common measure of dependence between binary variables is Cohen's Kappa (Cohen, 1960),

$$\kappa(\beta) = \frac{P_A - P_E}{1 - P_E} \quad (7)$$

where P_A is the joint probability of agreement and P_E is the joint probability of agreement under an assumption of independence. For the spatial model, we get

$$\begin{aligned} P_A(\beta) &= 1 - 2 \exp \left\{ -\frac{1}{\beta} \right\} + 2 \exp \left\{ -\frac{\vartheta(\mathbf{s}_1, \mathbf{s}_2)}{\beta} \right\} \\ P_E(\beta) &= 1 - 2 \exp \left\{ -\frac{1}{\beta} \right\} + 2 \exp \left\{ -\frac{2}{\beta} \right\}, \end{aligned}$$

and

$$\kappa(\beta) = \frac{P_A(\beta) - P_E(\beta)}{1 - P_E(\beta)} = \frac{\exp \left\{ -\frac{\vartheta(\mathbf{s}_1, \mathbf{s}_2) - 1}{\beta} \right\} - \exp \left\{ -\frac{1}{\beta} \right\}}{1 - \exp \left\{ -\frac{1}{\beta} \right\}} \quad (8)$$

where $\vartheta(\mathbf{s}_i, \mathbf{s}_j) = \sum_{l=1}^L [w_l(\mathbf{s}_i)^{1/\alpha} + w_l(\mathbf{s}_j)^{1/\alpha}]^\alpha$ is the pairwise extremal coefficient given by Reich and

Shaby (2012). To measure extremal dependence, let β go to ∞ so that events are increasingly more rare.

Then as shown in Appendix ??,

$$\kappa = \lim_{\beta \rightarrow \infty} \kappa(\beta) = 2 - \vartheta(\mathbf{s}_1, \mathbf{s}_2) \quad (9)$$

which is the same as the χ statistic of Coles et al. (1999), a commonly used measure of extremal dependence.

5 Computation

For small K we can evaluate the likelihood directly. When K is large, we use MCMC methods with the random effects model to explore the posterior distribution. This is possible because the expression for the joint density, conditional on A_1, \dots, A_L , is given by

$$P[Y(\mathbf{s}_1) = y(\mathbf{s}_1), \dots, Y(\mathbf{s}_n) = y(\mathbf{s}_n)] = \prod_{i=1}^n \pi(\mathbf{s}_i)^{1-Y_i} [1 - \pi(\mathbf{s}_i)]^{Y_i}. \quad (10)$$

where $\pi(\mathbf{s}_i)$ is given in (3). The model parameters and random effects are updated using a combination of Metropolis Hastings (MH) and Hamiltonian Monte Carlo (HMC) update steps. To overcome challenges with evaluating the positive stable density, we follow Reich and Shaby (2012) and incorporate the auxiliary variable technique of Stephenson (2009).

6 Simulation study

Needs updating For our simulation study, we generate $n_m = 50$ datasets under 6 different settings to explore the impact of sample size and misspecification of link function. We generate data assuming three possible types of underlying process. For each process, we consider two sample sizes $n_s = 650$ and $n_s = 1300$.

The first of these processes is a max-stable process that uses the GEV link described in (1) with knots on a 21×21 grid on $[0, 1] \times [0, 1]$. For this process, we set $\alpha = 0.3$, $\rho = 0.025$, $\xi = 0$ for identifiability purposes, and β_0 is set for each dataset to give 5% rarity. We then set $Y(\mathbf{s}) = I[z(\mathbf{s}) > 0]$ where $I[\cdot]$ is an indicator function.

For the second process, we generate a latent variable from a spatial Gaussian process with a mean of

96 $\text{logit}(0.05) \approx -2.9444$ and an exponential covariance given by

$$\text{cov}(\mathbf{s}_1, \mathbf{s}_2) = \tau_{\text{Gau}}^2 * \exp \left\{ -\frac{\|\mathbf{s}_1 - \mathbf{s}_2\|}{\rho_{\text{Gau}}} \right\} \quad (11)$$

97 where $\tau_{\text{Gau}} = 7$ and $\rho_{\text{Gau}} = 0.10$. The mean of the Gaussian process is set to give approximately 5% rarity.

98 Finally, we generate $Y(\mathbf{s}) \stackrel{\text{ind}}{\sim} \text{Bern}[\pi(\mathbf{s})]$ where $\pi(\mathbf{s}) = \exp \left\{ \frac{z(\mathbf{s})}{1+z(\mathbf{s})} \right\}$

99 For the third process, we generate data using a hotspot method. For this process, we first generate
 100 hotspots throughout the space, and then set the probability of occurrence to be higher when a site is within
 101 a circle of radius $\rho = 0.05$ from a hotspot location. More specifically, generate $K \sim \text{Poisson}(9)$ hotspot
 102 locations, $\mathbf{v}_1^*, \dots, \mathbf{v}_K^*$, from a uniform distribution over $[0, 1] \times [0, 1]$. If $\|\mathbf{s}_i - \mathbf{v}_k^*\| < 0.05$ for any k , then
 103 $\pi(\mathbf{s}_i) = 0.70$ otherwise, $\pi(\mathbf{s}_i) = 0.01$. We then generate $Y(\mathbf{s}_i) \stackrel{\text{ind}}{\sim} \text{Bern}[\pi(\mathbf{s}_i)]$.

104 For each dataset, we fit the model using three different methods, spatial logistic regression, spatial probit
 105 regression, and the proposed spatial GEV method.

106 6.1 Spatial logistic and probit methods

107 Because logistic and probit methods represent two of the more common spatial techniques for binary data,
 108 we chose to compare our method to them. One way these methods differ from our proposed method is
 109 that they assume the underlying process is Gaussian. In this case, we assume that $Z(\mathbf{s})$ follows a Gaussian
 110 process with mean $\mathbf{X}(s)^T \boldsymbol{\beta}$ and exponential covariance function. The marginal distributions are given by

$$P(Y = 1) = \begin{cases} \frac{\exp[\mathbf{X}^T \boldsymbol{\beta} + \mathbf{W} \boldsymbol{\alpha}]}{1 + \exp[\mathbf{X}^T \boldsymbol{\beta} + \mathbf{W} \boldsymbol{\alpha}]}, & \text{logistic} \\ \phi(\mathbf{X}^T \boldsymbol{\beta} + \mathbf{W} \boldsymbol{\alpha}), & \text{probit} \end{cases} \quad (12)$$

111 where $\boldsymbol{\alpha}$ are Gaussian random effects at the knot locations, and the \mathbf{W} are basis functions to recreate the
 112 Gaussian process at all sites.

6.2 Cross validation

Needs updating For each dataset, we fit the model using 500 of the observations as a training set, and the remaining observations are used as a validation set to assess the model’s predictive power. Because our goal is to predict a the occurrence of an event, we use Brier scores to compare the models (Gneiting and Raftery, 2007). The Brier score for predicting an occurrence at site \mathbf{s} is given by $\{I[Y(\mathbf{s}) = 1] - P[Y(\mathbf{s}) = 1]\}^2$ where $I[Y(\mathbf{s}) = 1]$ is an indicator function indicating that an event occurred at site \mathbf{s} , and $P[Y(\mathbf{s}) = 1]$ is obtained by taking the median of the posterior distribution. We average the Brier scores over all test sites, and a lower score indicates a better fit.

We also consider the receiver operating characteristic (ROC) curve, precision recall curve, as well as the area under the ROC curve (AUROC) for the different methods and settings. The ROC and PRC curves are computed using the ROCR (Sing et al., 2005) package in R (R Core Team, 2016) using the mean of the posterior predictive distribution at the testing locations. We then average AUCs across all datasets for each method and setting to obtain a single AUC for each combination of method and setting.

6.3 Results

Needs updating

Table Table 1 gives the Brier score relative to the Brier score for the spatial logistic method calculated as

$$BS_{\text{rel}} = \frac{BS_{\text{method}}}{BS_{\text{logistic}}}. \quad (13)$$

Table 2 gives the AUC relative to the AUC for the spatial logistic method calculated in similarly to the relative Brier score.

Table 1: Relative Brier scores for GEV and Probit methods

	GEV	Probit
Setting 1	0.9047	0.9754
Setting 2	0.7885	0.9804
Setting 3	1.0275	1.0018
Setting 4	1.0264	1.0089
Setting 5	1.0458	0.9963
Setting 6	1.0565	0.9945

Table 2: Relative AUC for GEV and Probit methods

	GEV	Probit	Logit
Setting 1	0.8998	0.8973	0.8897
Setting 2	0.9458	0.9399	0.9356
Setting 3	0.7288	0.7371	0.7157
Setting 4	0.7906	0.8056	0.8115
Setting 5	0.8426	0.8458	0.8388
Setting 6	0.8756	0.8686	0.8765

We analyzed the results for this simulation study using a Friedman test at $\alpha = 0.05$ to see if at least one method had a significantly different Brier score or AUC. For any setting that yielded a significant p-value, we conducted a Wilcoxon-Nemenyi-McDonald-Thompson test to see which of the methods had different results. The full results for the Wilcoxon-Nemenyi-McDonald-Thompson tests are given in Appendix A.3. For all settings, we find significant results for the Friedman test comparing the Brier scores for the methods. Specifically, we see a statistically significant reduction in Brier score using the GEV compared to logit for settings one and two and compared to probit for setting two. However, in the other settings, the logit and probit methods tend to perform better than the GEV method.

The results using AUC are much less conclusive with only settings one and four demonstrating significant differences between the methods at $\alpha = 0.05$. As with the Brier scores, the GEV method shows a statistically significant increase in AUC over the logit method for setting one, and for setting four, the both the probit and logit methods show a statistically significant improvement in AUC over the GEV method.

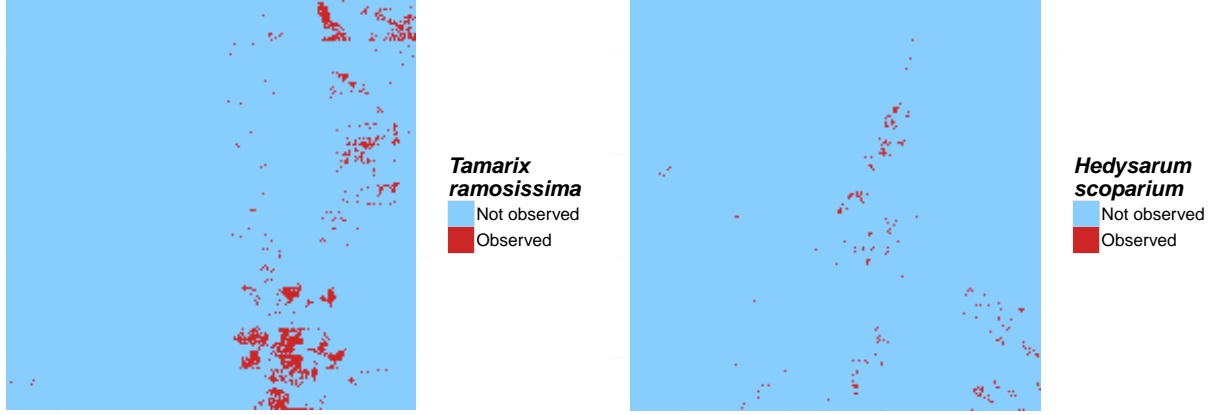


Figure 1: True occupancy of *Tamarix ramosissima* (left) and *Hedysarum scoparium* (right) from a 1-km² study region of PR China.

7 Data analysis

Needs updating

We compare our method to the spatial probit and logit for mapping the probability of the occurrence of two plant species, *Tamarix ramosissima* and *Hedysarum scoparium*, for a 1-km² study region of PR China Smith et al. (2012). The Chinese Academy of Forestry conducted a full census of the area, and the true occupancy of the species are plotted in Figure 1. The region is split into 5-m \times 5-m grid cells. *Tamarix ramosissima* can be found in 2.84% of the grid cells, and *Hedysarum scoparium* can be found in 0.54% of the grid cells. We subsample the original data using $n = 100$ or 250 initial locations for two different sampling design. The first is a two-stage spatially-adaptive cluster technique (CLU) taken from Pacifici et al. (2016). In this design, if an initial location is occupied, we also include the four rook neighbor (north, east, south, and west) sites in the sample. For the second design, we use a simple random sample (SRS) with the same number of sites included in the cluster sample.

For all models, knots are placed at all the grid cells in the sample. Additionally, for all models we only include an intercept term β_0 in the model, and the prior for the intercept is $\beta_0 \sim N(0, 10)$. For the spatial GEV model, we first fit a pairwise likelihood to obtain estimates $\hat{\rho}$, and $\hat{\alpha}$ which are used as starting values

159 in the MCMC sampler. The bandwidth parameter has prior $\log(\rho) \sim N(-3, 0.7)$, and α has a beta prior
 160 with mean $\hat{\alpha}$ and standard deviation 0.05. As with the simulation study, we fix $\xi = 0$ because we do not
 161 include any covariates.

162 For the spatial probit model, the bandwidth parameter has prior $\log(\rho) \sim N(-1, 2)$, and the prior on
 163 the variance term for the random effects is $IG(0.1, 0.1)$ where $IG(\cdot)$ is an Inverse Gamma distribution. For
 164 the spatial logit model, the bandwidth parameter has prior $Unif(0.001, 10)$, the prior on the variance term
 165 for the random effects is $IG(1, 1)$. Both the spatial probit and logit models assume an exponential covariance
 166 structure.

167 For all models, we run the MCMC sampler for 25,000 iterations with a burn-in period of 20,000 itera-
 168 tions. Convergence is assessed through visual inspection of traceplots.

169 **8 Conclusions**

170 **Acknowledgments**

171 **A Appendices**

172 **A.1 Binary regression using the GEV link**

173 Here, we provide a brief review of the the GEV link of Wang and Dey (2010). Let $Y_i \in \{0, 1\}, i = 1, \dots, n$
 174 be a collection of i.i.d. binary responses. It is assumed that $Y_i = I(z_i > 0)$ where $I(\cdot)$ is an indicator
 175 function, $z_i = [1 - \xi \mathbf{X}_i \boldsymbol{\beta}]^{1/\xi}$ is a latent variable following a $GEV(1, 1, 1)$ distribution, \mathbf{X}_i is the associated
 176 p -vector of covariates with first element equal to one for the intercept, and $\boldsymbol{\beta}$ is a p -vector of regression
 177 coefficients. Then, $Y_i \stackrel{ind}{\sim} \text{Bern}(\pi_i)$ where $\pi_i = 1 - \exp\left(-\frac{1}{z_i}\right)$.

178 A.2 Derivation of the likelihood

179 We use the hierarchical max-stable spatial model given by Reich and Shaby (2012). If at each margin, $Z_i \sim$
 180 $\text{GEV}(1, 1, 1)$, then $Z_i|\theta_i \stackrel{\text{indep}}{\sim} \text{GEV}(\theta, \alpha\theta, \alpha)$. We reorder the data such that $Y_1 = \dots = Y_K = 1$, and
 181 $Y_{K+1} = \dots = Y_n = 0$. Then the joint likelihood conditional on the random effect θ is

$$\begin{aligned}
 P(Y_1 = y_1, \dots, Y_n = y_n) &= \prod_{i \leq K} \left\{ 1 - \exp \left[- \left(\frac{\theta_i}{z_i} \right)^{1/\alpha} \right] \right\} \prod_{i > K} \exp \left[- \left(\frac{\theta_i}{z_i} \right)^{1/\alpha} \right] \\
 &= \exp \left[- \sum_{i=K+1}^n \left(\frac{\theta_i}{z_i} \right)^{1/\alpha} \right] - \exp \left[- \sum_{i=K+1}^n \left(\frac{\theta_i}{z_i} \right)^{1/\alpha} \right] \sum_{i=1}^K \exp \left[- \left(\frac{\theta_i}{z_i} \right)^{1/\alpha} \right] \\
 &\quad + \exp \left[- \sum_{i=K+1}^n \left(\frac{\theta_i}{z_i} \right)^{1/\alpha} \right] \sum_{1 < i < j \leq K} \left\{ \exp \left[- \left(\frac{\theta_i}{z_i} \right)^{1/\alpha} - \left(\frac{\theta_j}{z_j} \right)^{1/\alpha} \right] \right\} \\
 &\quad + \dots + (-1)^K \exp \left[- \sum_{i=1}^n \left(\frac{\theta_i}{z_i} \right)^{1/\alpha} \right]
 \end{aligned} \tag{14}$$

182 Finally marginalizing over the random effect, we obtain

$$\begin{aligned}
 P(Y_1 = y_1, \dots, Y_n = y_n) &= \int G(\mathbf{z}|\mathbf{A})p(\mathbf{A}|\alpha)d\mathbf{A}. \\
 &= \int \exp \left[- \sum_{i=K+1}^n \left(\frac{\theta_i}{z_i} \right)^{1/\alpha} \right] - \exp \left[- \sum_{i=K+1}^n \left(\frac{\theta_i}{z_i} \right)^{1/\alpha} \right] \sum_{i=1}^K \exp \left[- \left(\frac{\theta_i}{z_i} \right)^{1/\alpha} \right] \\
 &\quad + \exp \left[- \sum_{i=K+1}^n \left(\frac{\theta_i}{z_i} \right)^{1/\alpha} \right] \sum_{1 < i < j \leq K} \left\{ \exp \left[- \left(\frac{\theta_i}{z_i} \right)^{1/\alpha} - \left(\frac{\theta_j}{z_j} \right)^{1/\alpha} \right] \right\} \\
 &\quad + \dots + (-1)^K \exp \left[- \sum_{i=1}^n \left(\frac{\theta_i}{z_i} \right)^{1/\alpha} \right] p(\mathbf{A}|\alpha)d\mathbf{A}.
 \end{aligned} \tag{15}$$

183 Consider the first term in the summation,

$$\begin{aligned}
\int \exp \left\{ - \sum_{i=K+1}^n \left(\frac{\theta_i}{z_i} \right)^{1/\alpha} \right\} p(\mathbf{A}|\alpha) d\mathbf{A} &= \int \exp \left\{ - \sum_{i=K+1}^n \left(\frac{\left[\sum_{l=1}^L A_l w_l(\mathbf{s}_i)^{1/\alpha} \right]^\alpha}{z_i} \right)^{1/\alpha} \right\} p(\mathbf{A}|\alpha) d\mathbf{A} \\
&= \int \exp \left\{ - \sum_{i=K+1}^n \sum_{l=1}^L A_l \left(\frac{w_l(\mathbf{s}_i)}{z_i} \right)^{1/\alpha} \right\} p(\mathbf{A}|\alpha) d\mathbf{A} \\
&= \exp \left\{ - \sum_{l=1}^L \left[\sum_{i=K+1}^n \left(\frac{w_l(\mathbf{s}_i)}{z_i} \right)^{1/\alpha} \right]^\alpha \right\}. \tag{16}
\end{aligned}$$

184 The remaining terms in equation (15) are straightforward to obtain, and after integrating out the random
185 effect, the joint density for $K = 0, 1, 2$ is given by

$$P(Y_1 = y_1, \dots, Y_n = y_n) = \begin{cases} G(\mathbf{z}) & K = 0 \\ G(\mathbf{z}_{(1)}) - G(\mathbf{z}) & K = 1 \\ G(\mathbf{z}_{(12)}) - G(\mathbf{z}_{(1)}) - G(\mathbf{z}_{(2)}) + G(\mathbf{z}) & K = 2 \end{cases} \tag{17}$$

186 where

$$G[\mathbf{z}_{(1)}] = P[Z(\mathbf{s}_2) < z(\mathbf{s}_2), \dots, Z(\mathbf{s}_n) < z(\mathbf{s}_n)]$$

$$G[\mathbf{z}_{(2)}] = P[Z(\mathbf{s}_1) < z(\mathbf{s}_1), Z(\mathbf{s}_3) < z(\mathbf{s}_3), \dots, Z(\mathbf{s}_n) < z(\mathbf{s}_n)]$$

$$G[\mathbf{z}_{(12)}] = P[Z(\mathbf{s}_3) < z(\mathbf{s}_3), \dots, Z(\mathbf{s}_n) < z(\mathbf{s}_n)].$$

187 Similar expressions can be derived for all K , but become cumbersome for large K .

188 A.3 Simulation study pairwise difference results

189 Needs updating

The following tables show the methods that have significantly different Brier scores when using a Wilcoxon-Nemenyi-McDonald-Thompson test. In each column, different letters signify that the methods have significantly different Brier scores.

Table 3: Pairwise BS comparisons

	Setting 1	Setting 2	Setting 3	Setting 4	Setting 5	Setting 6
Method 1	A	A	A	C	B	B
Method 2	A B	B	A	B	A	A
Method 3	B	B	A	A	A B	A

References

- Cohen, J. (1960) A Coefficient of Agreement for Nominal Scales. *Educational and Psychological Measurement*, **20**, 37–46.
- Coles, S., Heffernan, J. and Tawn, J. (1999) Dependence Measures for Extreme Value Analyses. *Extremes*, **2**, 339–365.
- Genton, M. G., Ma, Y. and Sang, H. (2011) On the likelihood function of Gaussian max-stable processes. *Biometrika*, **98**, 481–488.
- Gneiting, T. and Raftery, A. E. (2007) Strictly Proper Scoring Rules, Prediction, and Estimation. *Journal of the American Statistical Association*, **102**, 359–378.
- de Haan, L. (1984) A Spectral Representation for Max-stable Processes. *The Annals of Probability*, **12**, 1194–1204.
- Heagerty, P. and Lele, S. (1998) A Composite Likelihood Approach to Binary Spatial Data. *Journal of the American Statistical Association*, **1459**, 1099–1111.
- Huser, R. and Davison, A. C. (2014) Space-time modelling of extreme events. *Journal of the Royal Statistical Society: Series B (Statistical Methodology)*, **76**, 439–461.
- Pacifici, K., Reich, B. J., Dorazio, R. M. and Conroy, M. J. (2016) Occupancy estimation for rare species using a spatially-adaptive sampling design. *Methods in Ecology and Evolution*, **7**, 285–293.
- Padoan, S. A., Ribatet, M. and Sisson, S. A. (2010) Likelihood-Based Inference for Max-Stable Processes. *Journal of the American Statistical Association*, **105**, 263–277.
- R Core Team (2016) *R: A Language and Environment for Statistical Computing*. R Foundation for Statistical Computing, Vienna, Austria. URL <https://www.R-project.org/>.
- Reich, B. J. and Shaby, B. A. (2012) A hierarchical max-stable spatial model for extreme precipitation. *The Annals of Applied Statistics*, **6**, 1430–1451.

- 216 Sing, T., Sander, O., Beerenwinkel, N. and Lengauer, T. (2005) ROCR: visualizing classifier performance
217 in R. *Bioinformatics*, **21**, 3940–3941.
- 218 Smith, D. R., Yuancai, L., Walter, C. A. and Young, J. A. (2012) Incorporating predicted species distribution
219 in adaptive and conventional sampling designs. In *Design and Analysis of Long-term Ecological Mon-*
220 *itoring Studies* (eds. R. A. Gitzen, J. J. Millspaugh, A. B. Cooper and D. S. Licht), chap. 17, 381–396.
221 Cambridge University Press.
- 222 Stephenson, A. G. (2009) High-Dimensional Parametric Modelling of Multivariate Extreme Events. *Aus-*
223 *tralian & New Zealand Journal of Statistics*, **51**, 77–88.
- 224 Tawn, J. A. (1990) Modelling multivariate extreme value distributions. *Biometrika*, **77**, 245–253.
- 225 Thibaud, E. and Opitz, T. (2015) Efficient inference and simulation for elliptical Pareto processes.
226 *Biometrika*, **102**, 855–870.
- 227 Wadsworth, J. L. and Tawn, J. A. (2014) Efficient inference for spatial extreme value processes associated
228 to log-Gaussian random functions. *Biometrika*, **101**, 1–15.
- 229 Wang, X. and Dey, D. K. (2010) Generalized extreme value regression for binary response data: An appli-
230 cation to B2B electronic payments system adoption. *The Annals of Applied Statistics*, **4**, 2000–2023.